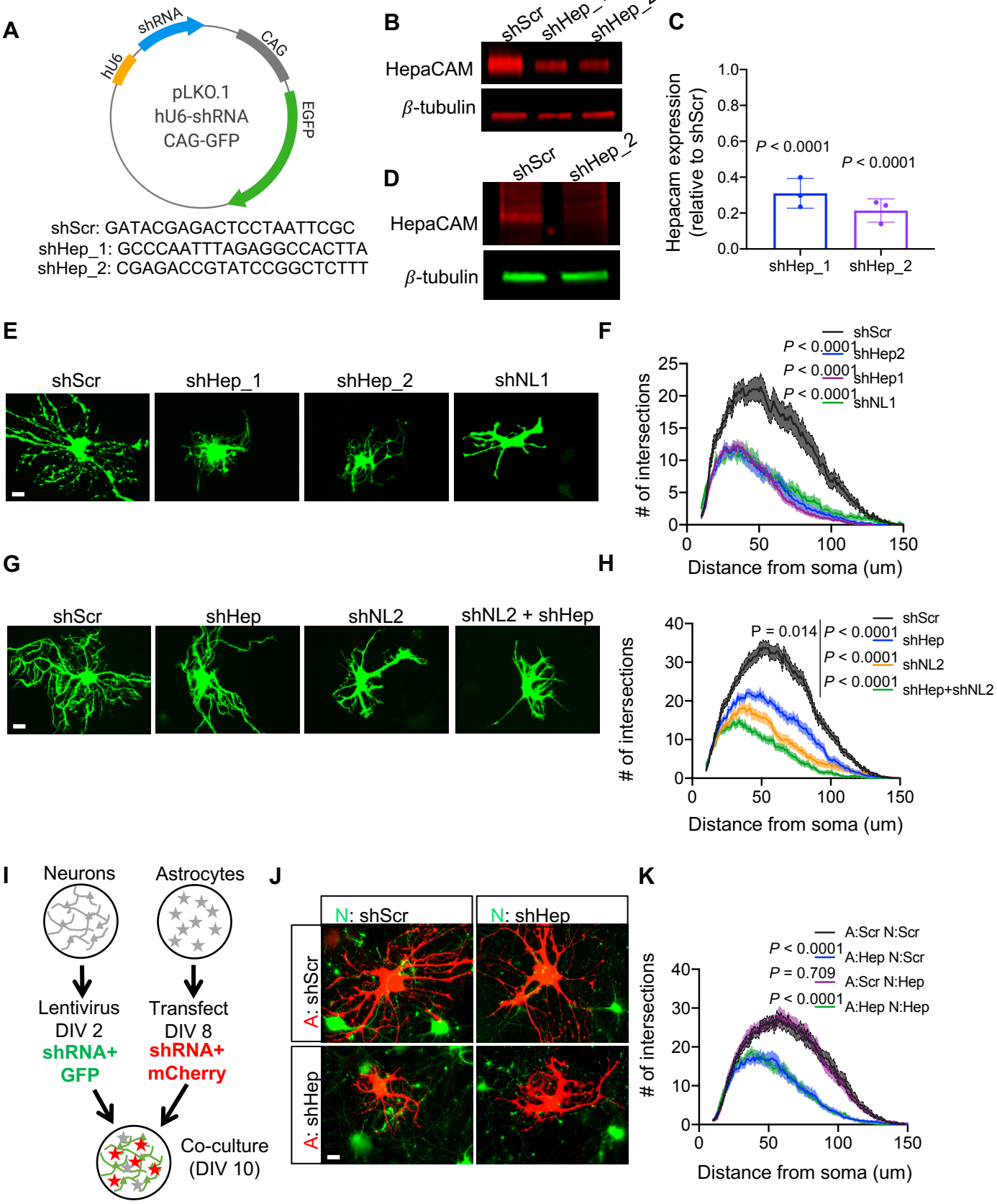
A
shRNA
CAG
hU6
EGFP
pLKO.1
hU6-shRNA
CAG-GFP
shScr: GATACGAGACTCCTAATTCGC
shHep_1: GCCCAATTTAGAGGCCACTTA
shHep_2: CGAGACCGTATCCGGCTCTTT
B
shScr
shHep_1
shHep_2
HepaCAM
β-tubulin
C
Hepacam expression (relative to shScr)
P < 0.0001
P < 0.0001
shHep_1
shHep_2
D
shScr
shHep_2
HepaCAM
β-tubulin
E
shScr
shHep_1
shHep_2
shNL1
F
shScr
shHep2
shHep1
shNL1
P < 0.0001
P < 0.0001
P < 0.0001
# of intersections
Distance from soma (um)
G
shScr
shHep
shNL2
shNL2 + shHep
H
shScr
shHep
shNL2
shHep+shNL2
P = 0.014
P < 0.0001
P < 0.0001
P < 0.0001
# of intersections
Distance from soma (um)
I
Neurons
Astrocytes
Lentivirus
DIV 2
shRNA+
GFP
Transfect
DIV 8
shRNA+
mCherry
Co-culture
(DIV 10)
J
N: shScr
N: shHep
A: shScr
A: shHep
K
A:Scr N:Scr
A:Hep N:Scr
A:Scr N:Hep
A:Hep N:Hep
P < 0.0001
P = 0.709
P < 0.0001
# of intersections
Distance from soma (um)

Figure S1. HepaCAM regulates astrocyte morphogenesis *in vitro*, Related to Figure 1. (A) Map of pLKO.1 plasmid expressing hU6-shRNA and CAG-EGFP. (B) Western blot of rat primary astrocytes transduced with lentivirus to express a scrambled shRNA (shScr) or one of two shRNAs targeting hepaCAM (shHep_1 or shHep_2) and treated with puromycin to deplete non-transduced cells. (C) Average protein expression in astrocytes expressing shHep_1 or shHep_2 normalized to β-tubulin and displayed relative to control protein levels (dotted line). Three independent experiments. One-way ANOVA, Dunnett's post-test. (D) Western blot of mouse primary astrocytes transduced with lentivirus to express shScr or shHep_2 (shHep). (E) Astrocytes transfected with shScr, shHep_1, shHep_2, or shRNA targeting NL1 (shNL1) and co-cultured with neurons. Scale bar, 20 μm. (F) Quantification of astrocyte branching complexity. n = 4 independent experiments, 20 cells/condition/experiment. ANCOVA, Tukey's post-test. (G) Astrocytes transfected with shScr, shHep, shNL2, or shNL2+shHep and co-cultured with neurons. Scale bar, 20 μm. (H) Quantification of astrocyte branching complexity. n = 3 independent experiments, 20 cells/condition/experiment. ANCOVA, Tukey's post-test. (I-K) hepaCAM does not regulate astrocyte morphogenesis via homophilic trans interaction with neurons. (I) Schematic of experiment. Neurons were transduced with lentivirus to express GFP and shHep or shScr. Astrocytes were transfected with plasmids expressing mCherry and shRNA and co-cultured with neurons for 48 hrs. (J) Images of astrocytes (red) co-cultured with neurons (green). Scale bar, 20 μm. (K) Quantification of astrocyte branching complexity. n = 4 independent experiments, 20 cells/condition/experiment. ANCOVA, Tukey's post-test. All graphs are mean ± s.e.m.

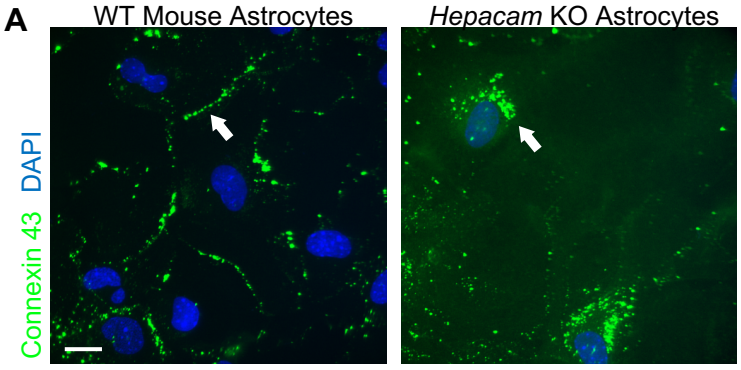
A
WT Mouse Astrocytes
Hepacam KO Astrocytes
Connexin 43
DAPI

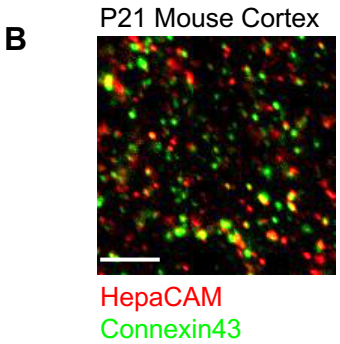
B
P21 Mouse Cortex
HepaCAM
Connexin43

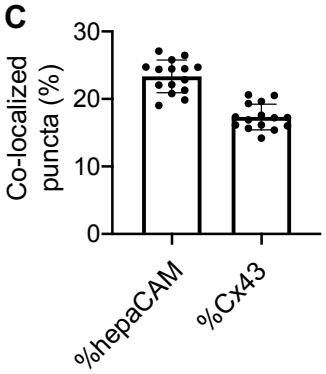
C
Co-localized puncta (%)
30
20
10
0
%hepaCAM
%Cx43

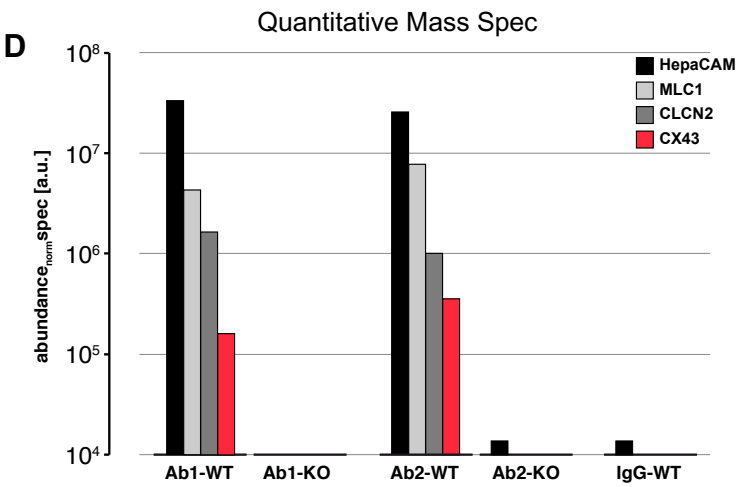
D
Quantitative Mass Spec
abundance_norm spec [a.u.]
10^8
10^7
10^6
10^5
10^4
HepaCAM
MLC1
CLCN2
CX43
Ab1-WT
Ab1-KO
Ab2-WT
Ab2-KO
IgG-WT

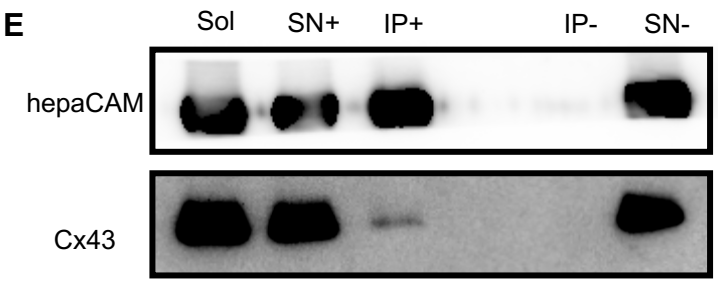
E
Sol
SN+
IP+
IP-
SN-
hepaCAM
Cx43

Figure S2. Specific co-purification of Cx43 with hepaCAM from mouse brain, Related to Figure 3. (A) Immunofluorescence of Cx43 in WT versus *Hepacam* KO mouse primary cultured astrocytes. In WT astrocytes, Cx43 is localized at cell membranes (arrow), whereas in the *HepaCAM* KO derived astrocytes, it is localized intracellularly (arrow). Scale bar, 10 µm. (B) Representative confocal microscopy image showing co-localization of hepaCAM (red) and Cx43 (green) in the neuropil of L5 of the V1 visual cortex. Scale bar, 20 µm. (C) Quantification of the percentage of hepaCAM puncta that are co-localized with Cx43 (% hepaCAM) and the percentage of Cx43 puncta that are co-localized with hepaCAM (%Cx43). n = 15 images from 3 mice. Data are means ± s.e.m. (D) Bar diagram showing the molecular abundances (at logarithmic scale) of the indicated proteins in a series of native affinity purifications analyzed by liquid chromatography-coupled high-resolution mass spectrometry (AP-MS). Two different anti-hepaCAM antibodies (a mouse monoclonal = Ab1 and a rabbit polyclonal = Ab2) were used together with a non-specific control IgG in APs from mouse wildtype (WT) and *Hepacam* knockout (KO) brain membranes solubilized with ComplexioLyte 47. Normalized protein abundances ($abundance_{norm}spec$ values) were calculated as the sum of all assigned and protein isoform-specific peptide ion intensities (PVs) divided by the number of MS-accessible protein isoform-specific amino acids(Bildl et al., 2012). Cx43 was found specifically and consistently co-purified with hepaCAM, although in lower amounts than the other two known hepaCAM-interacting proteins, MLC1 and CLC-2. MS noise levels in these experiments were in the range of 1000-10000 $abundance_{norm}spec$ units. (E) Western blot analysis of hepaCAM and Cx43 from solubilized brain membranes (Sol) and following co-immunoprecipitation with and antibody against hepaCAM (IP+). Cx43 is detected in the IP+, but not the IP- sample.

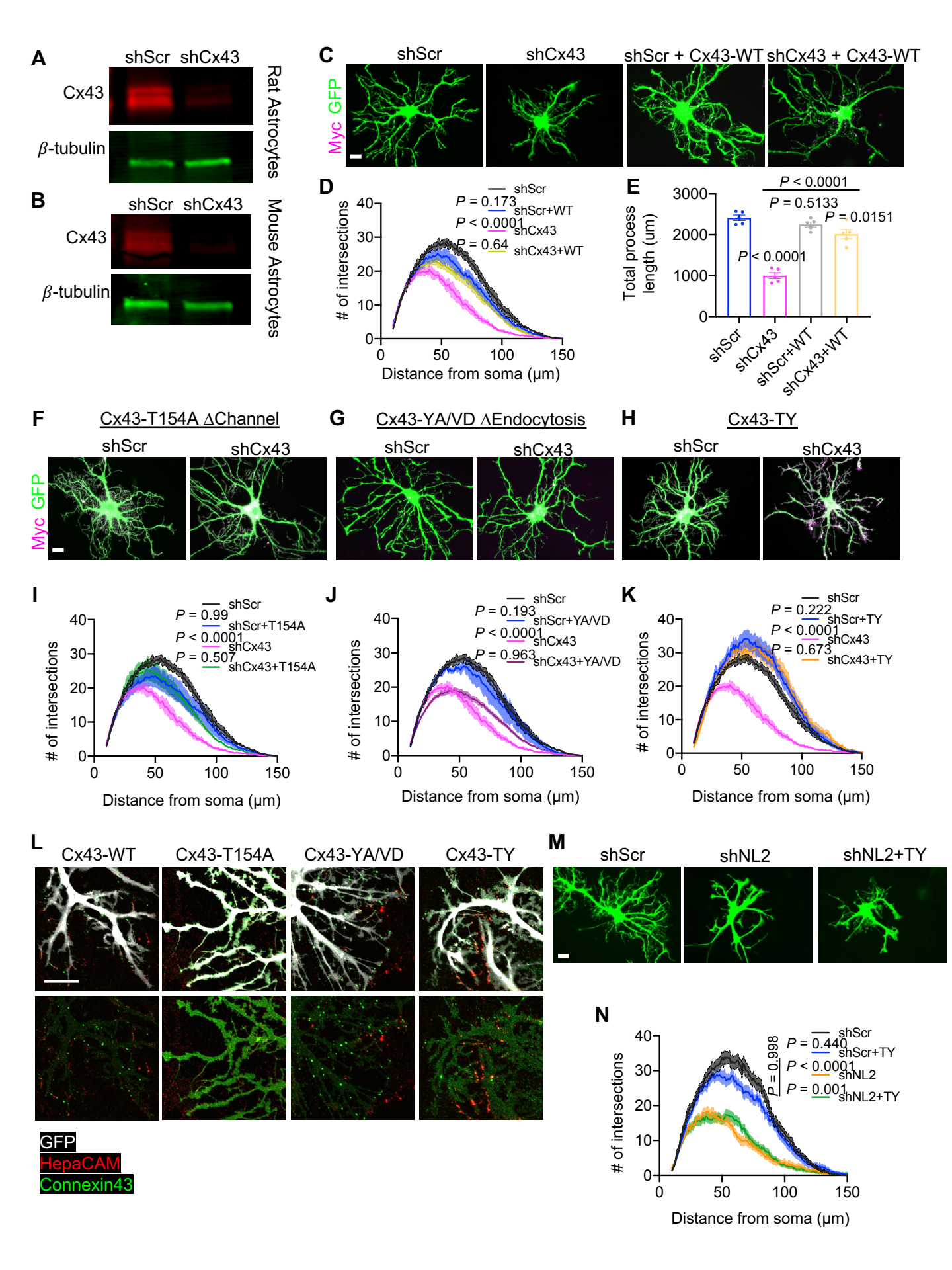
A
shScr shCx43
Cx43
β-tubulin
Rat Astrocytes
B
shScr shCx43
Cx43
β-tubulin
Mouse Astrocytes
C
shScr
shCx43
shScr + Cx43-WT
shCx43 + Cx43-WT
Myc GFP
D
shScr
P = 0.173 shScr+WT
P < 0.0001 shCx43
P = 0.64 shCx43+WT
# of intersections
Distance from soma (μm)
E
P < 0.0001
P = 0.5133
P = 0.0151
P < 0.0001
Total process length (um)
shScr
shCx43
shScr+WT
shCx43+WT
F
Cx43-T154A ΔChannel
shScr
shCx43
Myc GFP
G
Cx43-YA/VD ΔEndocytosis
shScr
shCx43
H
Cx43-TY
shScr
shCx43
I
shScr
P = 0.99 shScr+T154A
P < 0.0001 shCx43
P = 0.507 shCx43+T154A
# of intersections
Distance from soma (μm)
J
shScr
P = 0.193 shScr+YA/VD
P < 0.0001 shCx43
P = 0.963 shCx43+YA/VD
# of intersections
Distance from soma (μm)
K
shScr
P = 0.222 shScr+TY
P < 0.0001 shCx43
P = 0.673 shCx43+TY
# of intersections
Distance from soma (μm)
L
Cx43-WT
Cx43-T154A
Cx43-YA/VD
Cx43-TY
GFP
HepaCAM
Connexin43
M
shScr
shNL2
shNL2+TY
N
shScr
P = 0.440 shScr+TY
P = 0.998
P < 0.0001 shNL2
P = 0.001 shNL2+TY
# of intersections
Distance from soma (μm)

Figures S3. Cx43 regulates astrocyte morphogenesis *in vivo* through a channel-independent mechanism, Related to Figures 3 and 4. (A and B) Western blot of rat primary astrocytes (A) and mouse primary astrocytes (B) transduced with lentivirus to express a scrambled shRNA (shScr) or shRNA targeting Cx43 (shCx43) and treated with puromycin to deplete non-transduced cells. (C) Astrocytes (green) expressing shScr or shCx43 along with shRNA-resistant wild-type Cx43 (Cx43-WT) with a C-terminal myc tag (magenta) and co-cultured with neurons. Scale bar, 20 μm. (D) Quantification of astrocyte branching complexity. n = 3 independent experiments, 20 cells/condition/experiment. ANCOVA, Tukey's post-test. (E) Quantification of average total process length per astrocyte. n = 4 independent experiments, one-way ANOVA, Tukey's post-test. (F-H) Astrocytes (green) expressing shScr or shCx43 and Cx43-T154A (F), Cx43-YA/VD (G), or Cx43-TY (H) with a C-terminal myc tag (magenta). Scale bar, 20 μm. (I-K) Quantification of astrocyte branching complexity. n = 3 independent experiments, 20 cells/condition/experiment. ANCOVA, Tukey's post-test. For D, I, J, and K, the experiments were performed simultaneously using the same control conditions. Therefore, the same data for shScr and shCx43 are presented across multiple panels. (L) Astrocytes transfected with shScr-GFP and Cx43 mutant constructs, co-cultured with astrocytes and stained for GFP (gray), hepaCAM (red) and myc tag (green). Scale bar 20 μm. (M) Astrocytes co-cultured with neurons and expressing shScr, shNL2, or shNL2 and Cx43-TY. Scale bar, 20 μm. (N) Quantification of astrocyte branching complexity. n = 3 independent experiments, 20 cells/condition/experiment. ANCOVA, Tukey's post-test. All graphs are mean ± s.e.m.

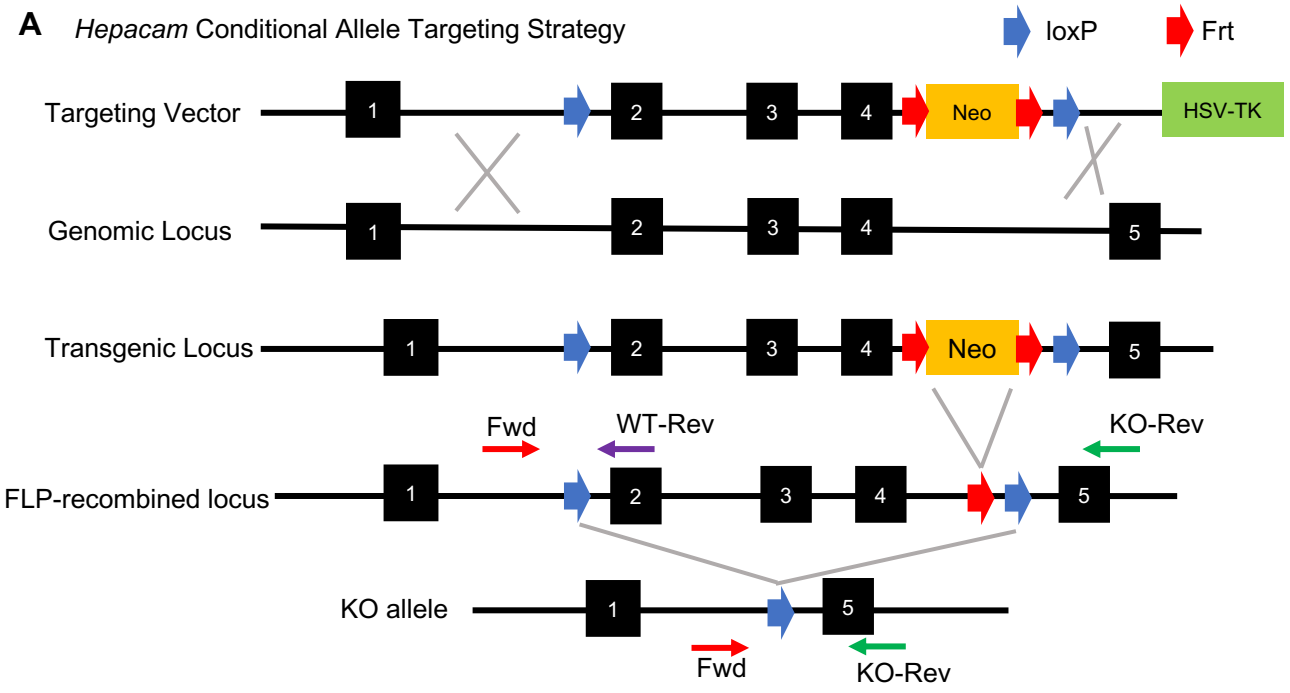
A
Hepacam Conditional Allele Targeting Strategy
loxP
Frt
Targeting Vector
Genomic Locus
Transgenic Locus
FLP-recombined locus
KO allele
Neo
HSV-TK
Fwd
WT-Rev
KO-Rev

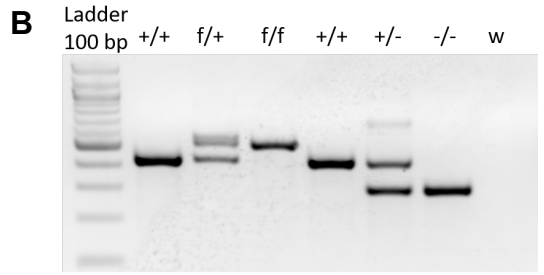
B
Ladder
100 bp
+/+
f/+
f/f
+/+
+/-
-/-
w

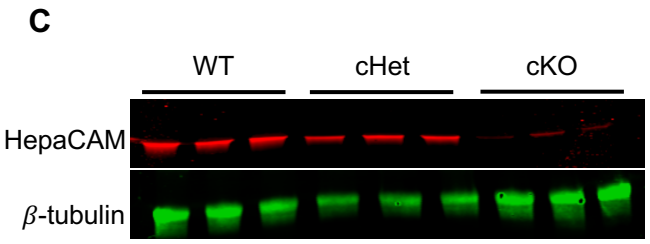
C
WT
cHet
cKO
HepaCAM
β-tubulin

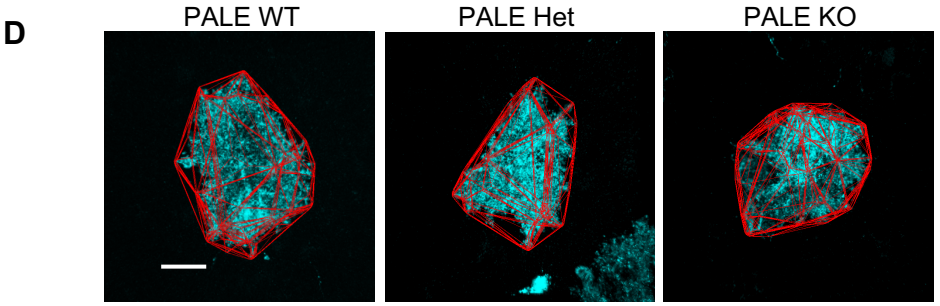
D
PALE WT
PALE Het
PALE KO

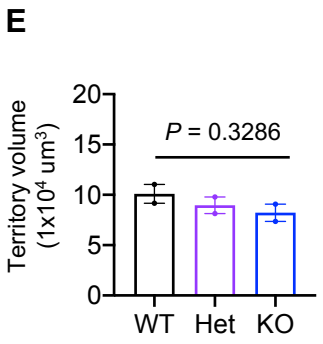
E
Territory volume
(1x10⁴ um³)
P = 0.3286
WT
Het
KO

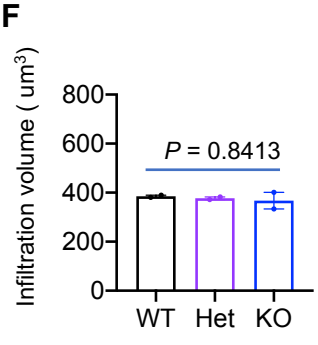
F
Infiltration volume (um³)
P = 0.8413
WT
Het
KO

Figure S4. Generation of a *Hepacam* conditional knockout mouse and confirmation of astrocyte-specific deletion in the mouse cortex, Related to Figure 5. (A) *Hepacam* conditional allele targeting strategy. Following recombination of the targeting vector with the genomic locus, germline transgenic mice were crossed with mice expressing the Gt(ROSA)26Sor$^{tm2(FLP*)Sor}$/J transgene (FLPo) to excise the Neo cassette and a generate a FLP-recombined locus. Cre-mediated recombination excises Exons 2-4 and generates a knockout allele. (B) PCR genotyping of genomic DNA from *Hepacam*$^{+/+}$, *Hepacam*$^{f/+}$, and *Hepacam*$^{f/f}$ mice using Fwd and WT-Rev primers which flank the 5' *loxp* site and generate a wild-type (WT) band of 443bp and a flox band of 532bp. To confirm Cre-mediate recombination, we crossed *Hepacam*$^{f/f}$ mice with transgenic CMV-Cre mice to generate *Hepacam* germline heterozygous (*Hepacam*$^{+/-}$) and knockout (*Hepacam*$^{-/-}$) mice. The Cre-recombined genomic locus was detected by Fwd and KO-Rev primers, producing a PCR band of 311bp. (C) Western blot analysis of cortical protein lysates from *Hepacam* WT, cHet, and cKO mice at P21. Each lane represents an independent mouse. Following normalization to β-tubulin, hepaCAM protein expression was not reduced in cHet mice compared to WT but was reduced by 86% in cKO mice. (D) Images of V1 L5 astrocytes from P21 *Hepacam*$^{+/+}$ (PALE WT), *Hepacam*$^{f/+}$ (PALE Het), and *Hepacam*$^{f/f}$ (PALE KO) mice labelled with td-Tomato (pseudo-colored cyan) from the Cre-dependent RTM transgene. (E) Average territory volume of td-Tomato+/Cre PALE astrocytes. Data points are mouse averages. Bars are mean ± s.e.m. n = 2 mice/condition, between 8-12 cells per mouse. Nested one-way ANOVA. Tukey's post-test. (F) Average neuropil infiltration volume at P21. Data points are mouse averages. Bars are mean ± s.e.m. n = 2 mice/condition, between 8-12 cells per mouse. Nested one-way ANOVA. Tukey's post-test.

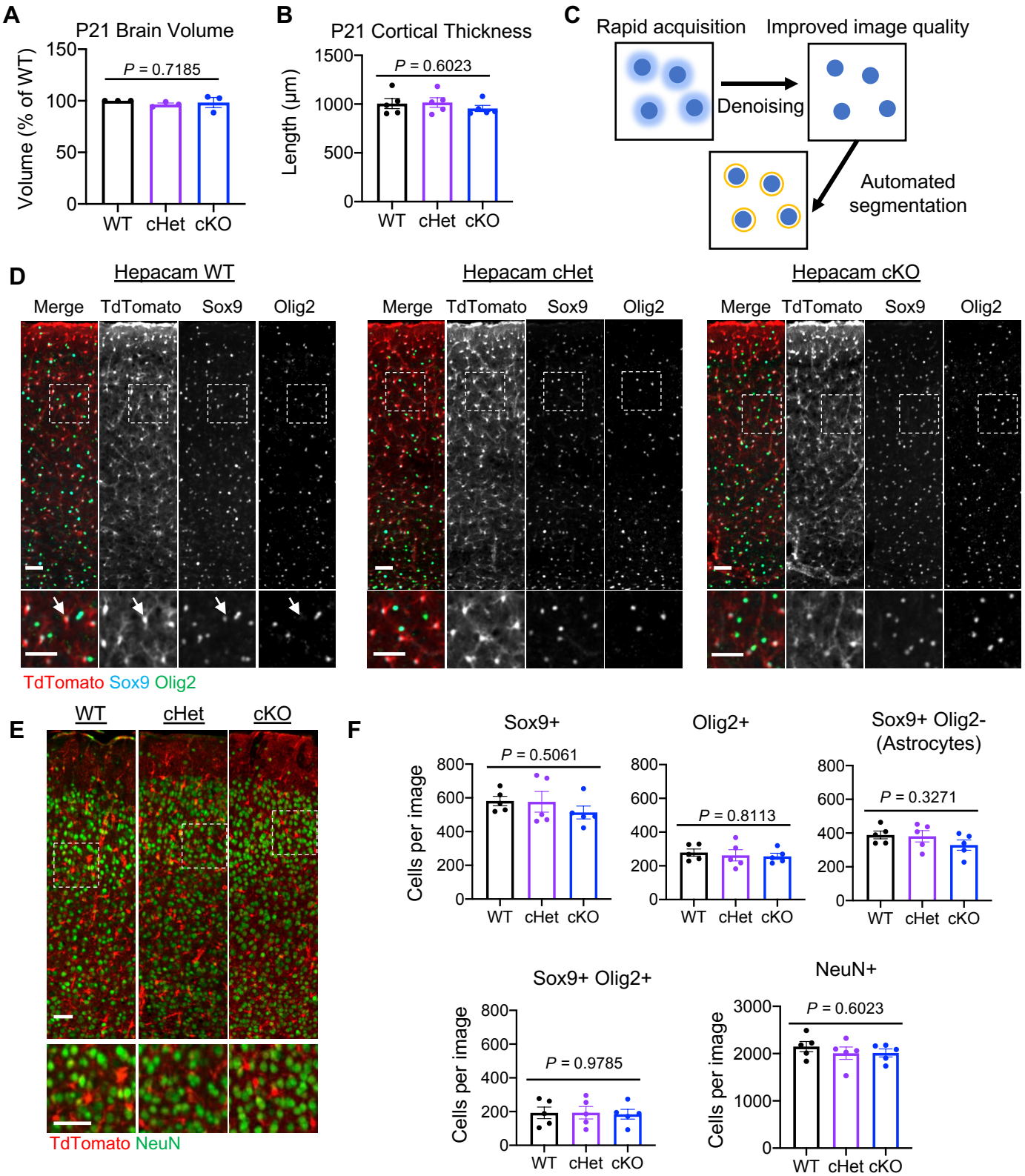
A
P21 Brain Volume
Volume (% of WT)
150
100
50
0
P = 0.7185
WT cHet cKO
B
P21 Cortical Thickness
Length (μm)
1500
1000
500
0
P = 0.6023
WT cHet cKO
C
Rapid acquisition
Improved image quality
Denoising
Automated segmentation
D
Hepacam WT
Hepacam cHet
Hepacam cKO
Merge TdTomato Sox9 Olig2
TdTomato Sox9 Olig2
E
WT cHet cKO
TdTomato NeuN
F
Sox9+
Olig2+
Sox9+ Olig2- (Astrocytes)
Sox9+ Olig2+
NeuN+
Cells per image
P = 0.5061
P = 0.8113
P = 0.3271
P = 0.9785
P = 0.6023
WT cHet cKO

Figure S5. Deletion of *Hepacam* from astrocytes does not alter brain size or cell number in the cortex at P21, Related to Figure 6. (A) Average volume of brains collected from *Hepacam* WT, cHet, and cKO mice following PFA perfusion at P21 and presented as a percentage of WT brain volume. n = 3 sex-matched littermate groups. Data points are mouse averages. Bars are mean ± s.e.m. One-way ANOVA. (B) Average thickness of the visual cortex at P21 measured from tile-scan confocal images. Measurement represents the distance in μm from the corpus callosum to the pial surface. 3 sex-matched littermate groups. 3 measurements per section, 3 sections per mouse. Data points are mouse averages. Bars are mean ± s.e.m. One-way ANOVA. (C) A schematic of the automated cell counting strategy using a machine learning-based method for image segmentation based on nuclear markers. (D) Images of P21 visual cortex from *Hepacam* WT, cHet, and cKO mice showing Cre-recombined cells (td-Tomato, red), Sox9+ cells (cyan) and Olig2+ cells (green). Sox9+ Olig2- labeling identifies astrocytes (arrows). Scale bars, 50 μm. (E) Images of P21 visual cortex from *Hepacam* WT, cHet, and cKO mice showing Cre-recombined cells (td-Tomato, red) and NeuN+ neurons (green). Scale bars, 50 μm. (F) Quantification of cell number based on nuclear markers. n = 5 sex-matched littermate groups. A total of 129,583 cells were counted amongst all genotypes, groups, and nuclear markers. Data points are mouse averages. Bars are mean ± s.e.m. One-way ANOVA.

A

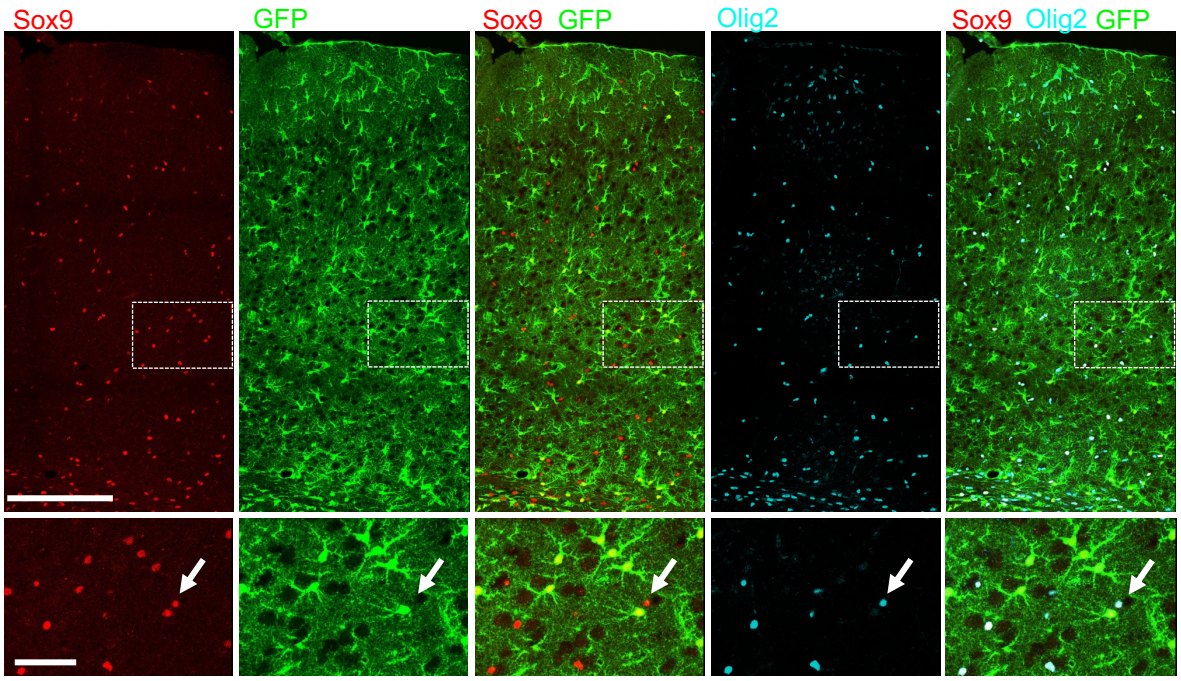

B

% GFP+ cells per nuclear marker category

	% GFP+	% GFP-
Sox9+	59.7	40.3
Olig2+	3.6	97.3
Sox9+/Olig2-	**96.8**	**3.2**
Sox9+/Olig2+	3.5	96.5
Sox9-/Olig2+	3.7	96.3

C

Identity of GFP+ cells

Sox9+/Olig2-	**89.9**
Sox9+/Olig2+	2.1
Sox9-/Olig2+	0.7
Sox9-/Olig2-	7.3

D

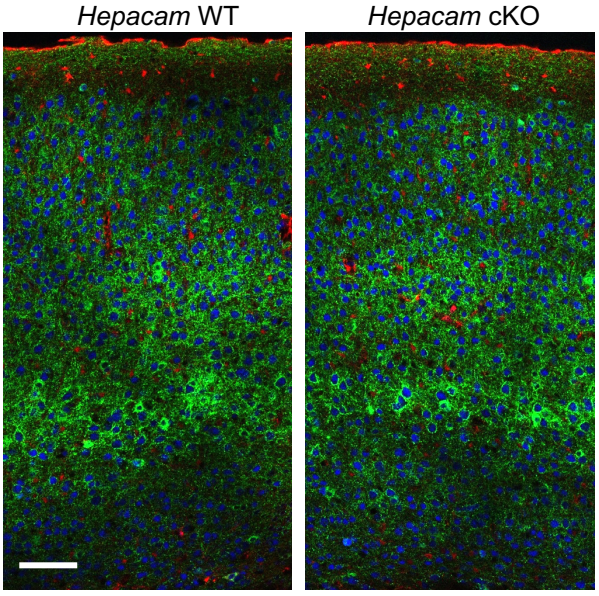

E

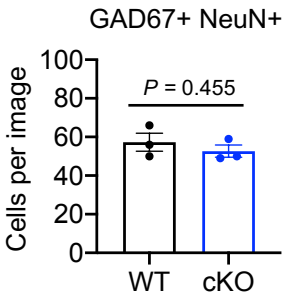

Figure S6. A nuclear labeling strategy to identify cortical astrocytes at P21, Related to Figure 6. (A) Confocal images of the visual cortex from P21 Aldh1l1-eGFP transgenic mice in which all astrocytes express GFP(Cahoy et al., 2008) (green) with labeling of Sox9 (red) and Olig2 (cyan). A previous study found that Sox9 is a specific nuclear marker for astrocytes in the adult brain (Sun et al., 2017). At P21 in the visual cortex, 90% of GFP+ astrocytes express Sox9. However, only 59.7% of Sox9+ cells are GFP+, suggesting that Sox9 labels a population of cells other than astrocytes at this age (arrows). Interestingly, 95% of GFP-/Sox9+ cells express the oligodendrocyte lineage marker Olig2 at P21, and only 3.5% of Sox9+/Olig2+ cells are also GFP+. Therefore, we used the classification of Sox9+/Olig2- to identify grey matter astrocytes in the mouse cortex at P21. (B) A summary of the percentage of cells expressing GFP for each nuclear marker category. (C) A summary of the nuclear label identity of GFP+ cells. Data were collected from 3 images per mouse, from 3 mice. (D) Representative single optical section confocal images of Hepacam WT and cKO cortices stained with NeuN and GAD67 to identify interneurons. Scale bar, 100 μm. (E) Quantification of average number of GAD67+ NeuN+ cells 10 μm z-stack, tile scan image. n = 3 sex-matched littermate pairs. Data points are mouse averages. Bars are mean ± s.e.m. Unpaired, two-tailed t test.

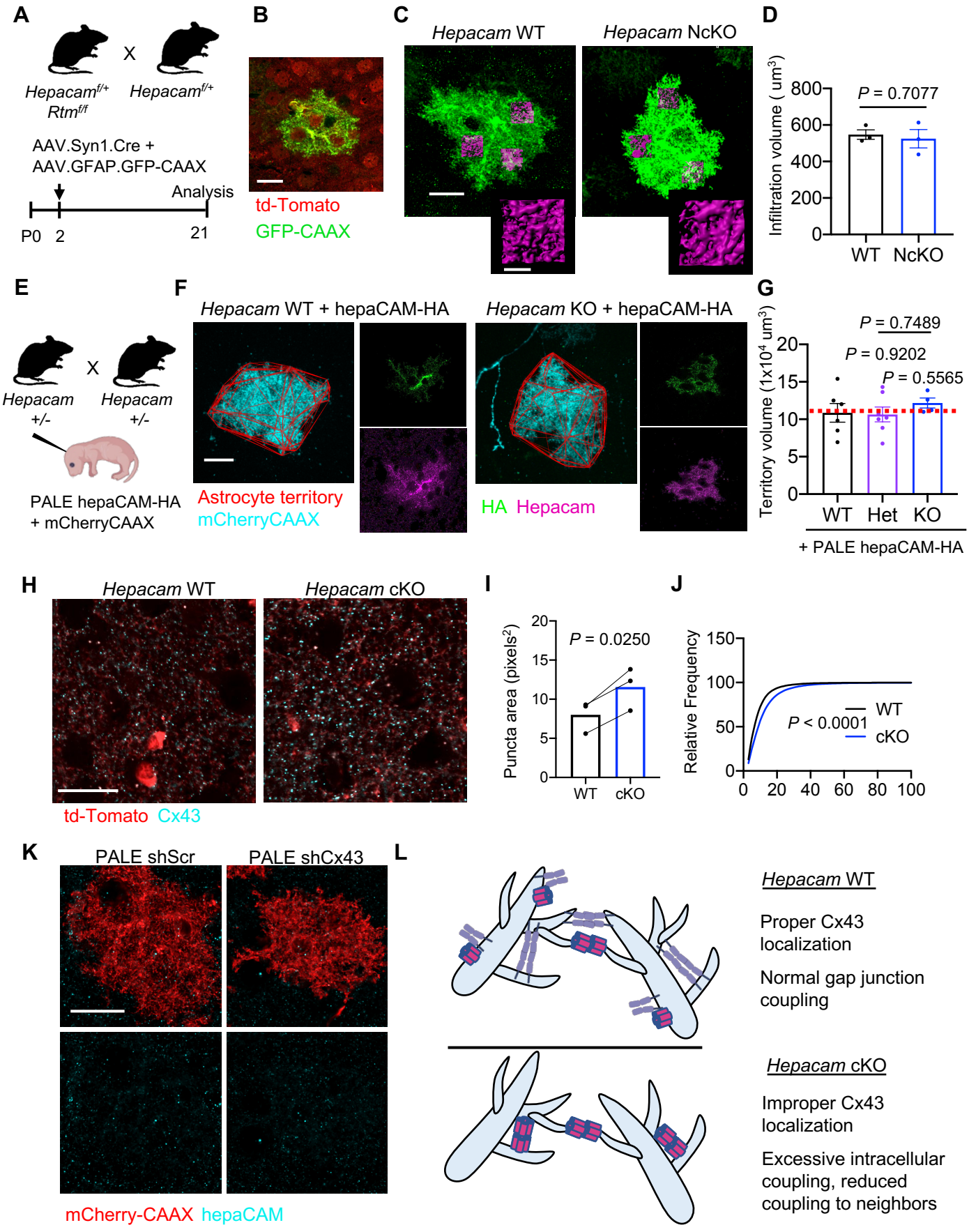
A
Hepacam f/+ Rtm f/f
X
Hepacam f/+
AAV.Syn1.Cre +
AAV.GFAP.GFP-CAAX
Analysis
P0 2 21
B
td-Tomato
GFP-CAAX
C
Hepacam WT
Hepacam NcKO
D
Infiltration volume (um3)
P = 0.7077
WT NcKO
E
Hepacam +/-
X
Hepacam +/-
PALE hepaCAM-HA
+ mCherryCAAX
F
Hepacam WT + hepaCAM-HA
Hepacam KO + hepaCAM-HA
Astrocyte territory
mCherryCAAX
HA Hepacam
G
Territory volume (1x10^4 um3)
P = 0.7489
P = 0.9202
P = 0.5565
WT Het KO
+ PALE hepaCAM-HA
H
Hepacam WT
Hepacam cKO
td-Tomato Cx43
I
Puncta area (pixels2)
P = 0.0250
WT cKO
J
Relative Frequency
P < 0.0001
WT
cKO
K
PALE shScr
PALE shCx43
mCherry-CAAX hepaCAM
L
Hepacam WT
Proper Cx43 localization
Normal gap junction coupling
Hepacam cKO
Improper Cx43 localization
Excessive intracellular coupling, reduced coupling to neighbors

Figures S7. HepaCAM overexpression does not alter astrocyte territory volume, Related to Figures 6 and 7. (A) Strategy for deletion of hepaCAM from astrocytes by P2 intracortical injection of PHP.eB2 serotype Adeno-associated virus (AAV) expressing Cre under control of the synapsin-1 (Syn1) promoter into the cortex of *Hepacam*$^{+/+}$ and *Hepacam*$^{f/+}$. Astrocytes were labeled with GFP-CAAX by simultaneous injection of AAV.GFAP.GFP-CAAX. (B) Evidence of successful targeting of neurons, visible via td-Tomato expression. (C) Images of GFP-CAAX-labeled astrocytes from *Hepacam* WT and *Hepacam* neuron cKO (NcKO) mice. Scale bar, 20 µm. Insets show NIV reconstructions (magenta). Scale bar, 5 µm. (D) Average NIV. 3 ROIs per cell, n = 3 mice/condition, between 4-10 cells mouse. Data points are mouse averages. Bars are mean ± s.e.m. Nested one-way ANOVA. Tukey's post-test. Data points are mouse averages, bars are mean ± s.e.m. (E) Strategy for overexpression of WT hepaCAM-HA in *Hepacam* WT, Het, and KO mice. (F) V1 L5 astrocytes from *Hepacam* WT and *Hepacam* KO astrocytes expressing mCherry-CAAX (cyan) and hepaCAM-HA (green). Territory volume in red and hepaCAM staining in magenta. Scale bar, 20 µm. (G) Quantification of astrocyte territory volume. The dotted red line represents the average territory volume of WT astrocytes expressing mCherry-CAAX from experiments in 1L, 3H, and 4E. n = 6 WT, 7 Het, and 4 KO mice, between 1-12 cells per mouse. Data points are mouse averages. Bars are mean ± s.e.m. Nested one-way ANOVA. Tukey's post-test. (H) Confocal images of Cx43 expression (cyan) in Hepacam WT and Hepacam cKO mice at P60. Scale bar, 20 µm. (I) Average Cx43 puncta size. 5 images per section, 3 sections per brain, from 3 sex-matched littermate pairs. Data points are mouse averages. Bars are mean ± s.e.m. Paired two-tailed t test. (J) Cumulative probability distribution of Cx43 puncta size. 5 images per section, 3 sections per mouse, 3 mice per genotype. Kolmogorov-Smirnov test. (K) Confocal images of P21 L5 V1 astrocytes expressing mCherry-CAAX and shScr or shCx43 and stained for hepaCAM (cyan). Scale bar, 20 µm. (L) Model of how loss of hepaCAM may alter Cx43 localization to impair gap junction coupling between neighboring astrocytes.

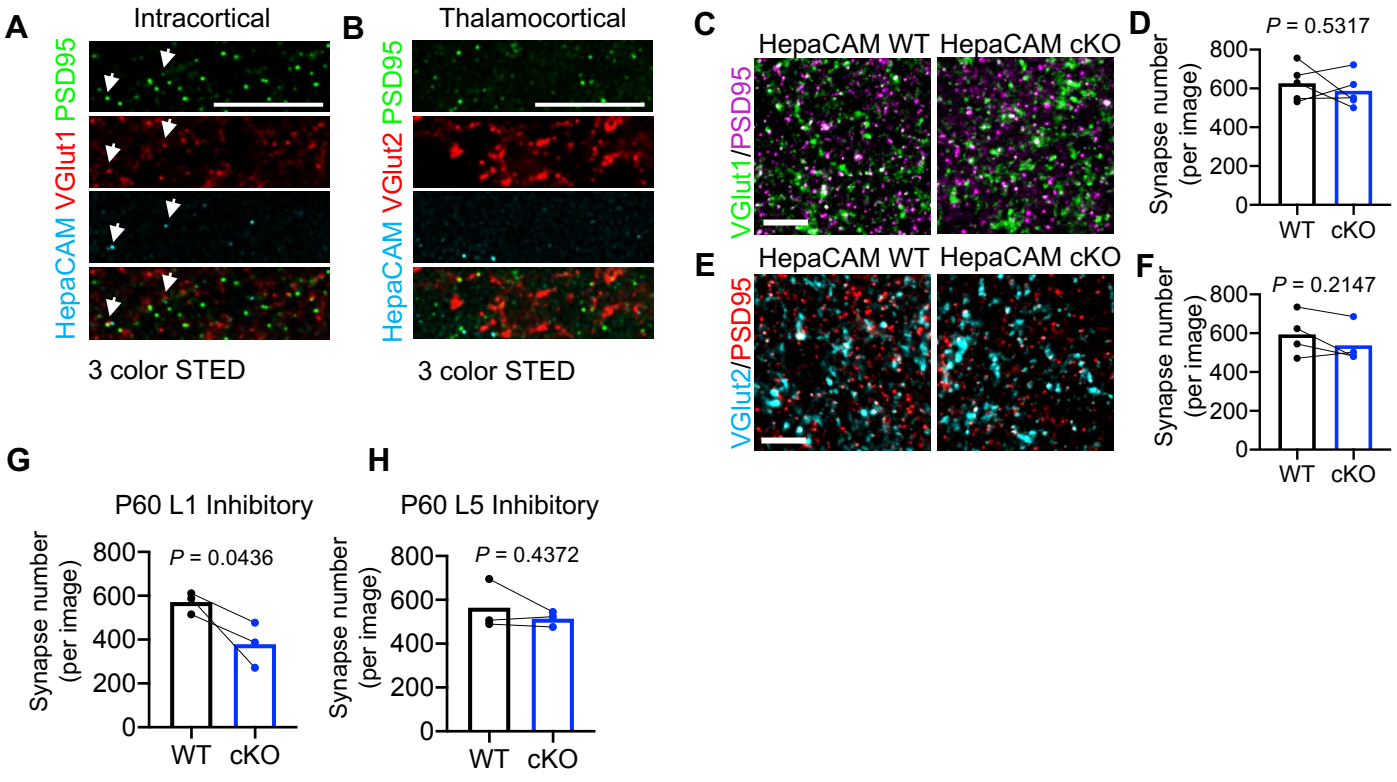
A
Intracortical
HepaCAM VGlut1 PSD95
3 color STED
B
Thalamocortical
HepaCAM VGlut2 PSD95
3 color STED
C
HepaCAM WT
HepaCAM cKO
VGlut1/PSD95
D
P = 0.5317
Synapse number (per image)
800
600
400
200
0
WT
cKO
E
HepaCAM WT
HepaCAM cKO
VGlut2/PSD95
F
P = 0.2147
Synapse number (per image)
800
600
400
200
0
WT
cKO
G
P60 L1 Inhibitory
Synapse number (per image)
P = 0.0436
800
600
400
200
0
WT
cKO
H
P60 L5 Inhibitory
Synapse number (per image)
P = 0.4372
800
600
400
200
0
WT
cKO

Figure S8. Astrocytic hepaCAM does not alter excitatory synapse number, Related to Figure 8. (A) Three-color STED image of hepaCAM (cyan) and excitatory intracortical synapses, labeled by presynaptic VGlut1 (red) and postsynaptic PSD95 (green) from L1 of V1 cortex at P21 in WT mice. HepaCAM is occasionally observed co-localized with excitatory intracortical synapses (arrows). (B) Representative three-color STED image of hepaCAM (cyan) and excitatory thalamocortical synapses, labeled by presynaptic VGlut2 (red) and postsynaptic PSD95 (green) from L1 of V1 cortex at P21 in WT mice. HepaCAM co-localization is rarely observed with thalamocortical synapses. (C) Excitatory intracortical synapses (VGlut1(green), PSD95 (magenta)) in L1 of V1 cortex at P21 in *Hepacam* WT and cKO mice. (D) Average number of excitatory intracortical synapses per image. 5 images per section, 3 sections per mouse, 5 sex-matched littermate pairs. Data points are animal averages, bars are mean ± s.e.m. Paired two-tailed t test. (E) Excitatory thalamocortical synapses (VGlut2 (cyan), PSD95 (red)) in L1 of V1 cortex at P21 in *Hepacam* WT and cKO mice. (F) Average number of excitatory thalamocortical synapses per image. 5 images per section, 3 sections per mouse, 4 sex-matched littermate pairs. Data points are animal averages, bars are mean ± s.e.m. Paired two-tailed t test. All scale bars, 5 μm. (G, H) Number of inhibitory synapses in L1 (G) and L5 (H) of the V1 cortex at P60. 5 images per section, 3 sections per mouse, 3 sex-matched littermate pairs. Data points are animal averages, bars are mean ± s.e.m. Paired two-tailed t test.

Primer Name	Source	Sequence (5' - 3')
Hepacam WT Fwd	This paper	TACCCAGCCAATAAGGAGTAGAC
Hepacam WT Rev	This paper	CATTGCCTGTCTTCTGCACTT
Hepacam KO Rev	This paper	GTAGGCTGTTCATTCAGTGTGAG
oIMR9020 (RTM WT Fwd)	Jackson	AAG GGA GCT GCA GTG GAG TA
oIMR9021 (RTM WT Rev)	Jackson	CCG AAA ATC TGT GGG AAG TC
oIMR9103 (RTM Mut Fwd)	Jackson	GGC ATT AAA GCA GCG TAT CC
oIMR9105 (RTM Mut Rev)	Jackson	CTG TTC CTG TAC GGC ATG G
30308 (Aldh1L1 Cre Fwd)	Jackson	GGC AAA CGG ACA GAA GCA
31091 (Aldh1L1 Cre Fwd)	Jackson	CTT CAA CAG GTG CCT TCC A
oIMR8052 (Flp Mut Rev)	Jackson	GCG AAG AGT TTG TCC TCA ACC
oIMR8545 (Flp Fwd)	Jackson	AAA GTC GCT CTG AGT TGT TAT
oIMR8546 (Flp WT Rev)	Jackson	GGA GCG GGA GAA ATG GAT ATG
Cre Fwd (EMX1-Cre)	Jackson	GCATTACCGGTCGATGCAACGAGTGATGA
Cre Rev (EMX1-Cre)	Jackson	GAGTGAACGAACCTGGTCGAAATCAGTGC
GT 294 (MADM)	Contreras et al., 2020	CCA AGC TGA AGG TGA CCA AG
GT 295 (MADM)	Contreras et al., 2020	TCT TCT TCT GCA TTA CGG GG
TG 159 (MADM)	Contreras et al., 2020	GGA CTG GGT GCT CAG GTA GTG GTT GTC G
TG 162 (MADM)	Contreras et al., 2020	GGT ACG TCC AGG AGC GCA CCA TCT TCT TCA AGG
Chr9 Fwd	Contreras et al., 2020	GGC CAA ACT AAC CCA AGC AG
Chr9 Rev	Contreras et al., 2020	TAG AGC CTC CTC CCA ACA CC
177 MADM Rev	Contreras et al., 2020	TCA ATG GGC GGG GGT CGT T

Table S1. PCR Genotyping Primers, Related to STAR Methods

Primer Name	Sequence (5' - 3')
pB-hU6 Fwd	GGACTAGTCAGGCCCGAAGGAATAGAAG
pB-hU6 Rev	GGACTAGTGCCAAAGTGGATCTCTGCTG
Forward_Hepa CAM_HA	ACAAAAGTTGTGATGTATCCATACGACGTTCCGGACTACGCATAGTAC CCAGCTTTCTTGTACAAAGTGGTTGATATCCAGCACAGTGGC
Reverse_Hepa CAM_HA	GAAAGCTGGGTACTATGCGTAGTCCGGAACGTCGTATGGATACATCA CAACTTTTGTATACAAAGTTGTGGCGCTGATCTCCACCGGGCC
Forward_Hepa CAM∆C_HA	ACAAAAGTTGTGATGTATCCATACGACGTTCCGGACTACGCATAGTAC CCAGCTTTCTTGTACAAAGTGGTTGATCCTCTCGAGCCTCTA
Reverse_Hepa CAM∆C_HA	GAAAGCTGGGTACTATGCGTAGTCCGGAACGTCGTATGGATACATCA CAACTTTTGTATACAAAGTTGTATCCATGTATTCCAGGGAGTT
Cx43_RM_Fwd	TGCACCTGAAGCAAATAGAGATTAAGAAGTTCAAGTACGGGATTG
Cx43_RM_Rev	CAATCCCGTACTTGAACTTCTTAATCTCTATTTGCTTCAGGTGCA
T154A_Fwd	GGCTTGCTGAGAGCCTACATCATCAGCATCCT
T154A_Rev	TGATGATGTAGGCTCTCAGCAAGCCGCCCCTC)

Table S2. Mutagenesis Primers, Related to STAR Methods